

# 3D Boundaries Partial Representatiton Of Objects using Interval Analysis

Benoit TELLE, Olivier STASSE, Toshio UESHIBA, Kazuhito YOKOI, and Fumiaki TOMITA  
 3D Vision Group and JRL (CNRS), Intelligent System Institute, AIST  
 1-1-4, Umezono  
 Tsukuba, 305-8568 Japan  
 Email: {telle, stasse, ueshiba, yokoi, tomita}@aist.go.jp

**Abstract**— This papers presents an application of Interval Analysis to a 3D reconstruction problem. The aim is to build a partial boundaries representation of an object including guaranteed information according to the camera model. Features points coordinates are described using intervals. This representation is used together with a method to search stereo correspondence based on the connectivity of segments.

## I. INTRODUCTION

This papers deals with the problem of error estimation in 3D reconstruction. In this problem, errors may arise from the physical camera in the choosen camera model, from the segmentation process, and from the pixel information. Error is usually taking into account through an additive term on estimated measures, i.e. the pixel information, or the parameters of the camera model or both. The most common form of this additive term is a Gaussian distribution. This model was used in common camera calibration process [1] [2]. Concerning applications, the mathematical tools provided by this model lead to numerous results, such as camera self-calibration and motion estimation [3], environment modeling [4], self localization applied to robots [5], registration [6], or visual servoing [7]. This model is based on several hypothesis such as centered distribution and indpendance variables. These hypothesis are known to be approximative, but as they are statistically representative of the physical model through numerous samples, they allow a good identification. However when considering 3D reconstruction, only a few number of variables is involved, and the true geometrical model of the camera becomes proeminent. A statistical study on the influence of modelization by Gaussian noise with different resolution can be find in [8], but it also possible to solve the 3D reconstruction problem based on geometrics consideration. Indeed, a new approach of the 3D reconstruction problem using Interval Analysis has been proposed in [9] and [10]. The novelty in this paper is to apply this approach to the first step of 3D object reconstruction, together with a very robust stereoscopic segments based correspondence method [11], and considering the new camera model.

The targeted application is 3D objet modelling for the HRP-2 [12] humanoid robot. The created model could be used for two main tasks: visual-search and visual-servoing manipulation. Such model-creation capability is particulary usefull when the robot has to handle new objects for which no models has been provided. This is particulary true for

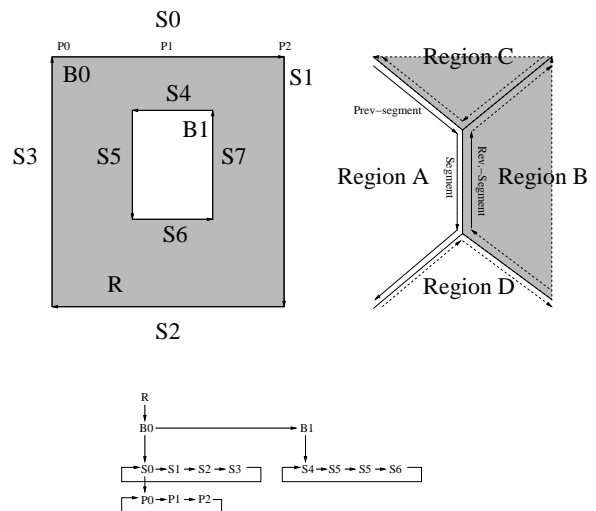


Fig. 1. B-rep data structure.

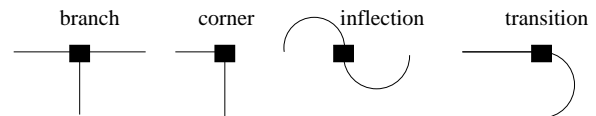


Fig. 2. End points of B-rep segments.

humanoid robots no-dedicated for one particular task, and evolving in open environments. A first step towards the manipulation of unknown objects is to deal with the error estimation of the knowledge we can have on this object.

The first section introduces the method used to build the boundary representation. The second section describes the interval analysis tools which are used in the context of 3D uncertainty computation. The third section presents the results applied to some objects relevant to the application context.

## II. THE VVV SYSTEM

### A. System configuration

The HRP-2 humanoid robot is equipped with a vision sytem called VVV [12]. This versatile system using a trinocular stereo camera setup is able to reconstruct 3D information of a scene, to recognise an object [13], to track a recognised object [14], and to build a model using a range finder system.

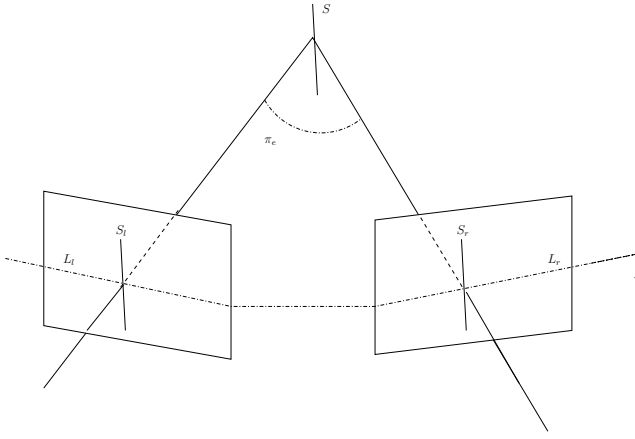


Fig. 3. Two matched segments ( $S_l, S_r$ ) and epipolar constraint allows to compute matched points through the intersection of epipolar line ( $L_l, L_r$ ) and segments ( $S_l, S_r$ ).

### B. Boundary representation of an Image

In the VVV system, an image is described using boundary representation. This boundary representation is build after performing an edge detection using a Sobel and a Laplacian operators. The result is divided in segments linked using four types of characteristics points : *branch*, *corner*, *inflection* and *transition*. The first two kinds deal with straight segments, whereas inflection and transition points deal with curved segments. Inflection points describe changes in the curvature sign, and the transition describe a change from zero to non-zero value for the curvature.

The segments linked one to the others define boundaries, which in turn define regions. Thus the corresponding data structure, called B-Rep, is made of four layers: *region* (R), *boundary* (B), *segment* (S) and *point*(P). The points at the beginning of each segments are the ones to which the interval analysis is applied. An example of the B-rep data structure is given in figure 1.

### C. Using boundary representation for matching

The boundary representation of an image pair allows the computation of robust matching between a left-right pair of images. As it is described in [11] segments' boundaries from the left image are compared with segments' boundaries from the right image using the epipolar condition and the segments characteristics: shape, intensity, direction and connectivity. Then, 2 bidimensionnal matched B-rep are equivalent to 2 set of matched segments in the images. On figure (3) we can see two matched segments ( $S_l, S_r$ ). Now, the epipolar constraint is used to find matched points. Epipolar line ( $L_l, L_r$ ) are the intersection of image plane and epipolar plane ( $\pi_e$ ). Intersections of segments with epipolar lines furnishe matched points in the image pair. These points will be used in 3D reconstruction. Moreover, in our context, a third camera is used to check the correctness of some matchings. The final output of this process is a partial 3-dimensional boundaries representation of the objects in the scene. These are visible in figures 6(a)(b)(c).

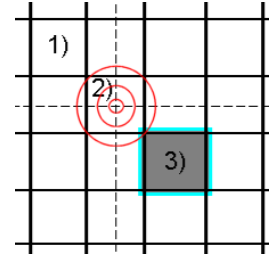


Fig. 4. 1) real pixel 2) probabilistic model of pixel 3) interval representation of pixel by an interval.

## III. CHOICE OF MODELS

### A. Camera model

The most popular camera model in computer vision is the pinhole model. It allows to use the projective geometry properties; thus the projection observed by a camera is a linear application given by equation (1). Dimensions of the matrix  $P_i$  are  $(3 \times 4)$ . This model has 12 degrees of freedom. The complete projection of a scene point through the camera model is given by:

$$q = PQ_h = K(R|t)Q_h \quad (1)$$

where  $K$  is the matrix of intrinsic parameters,  $(R|t)$  is the matrix of extrinsic parameters.  $R$  represents the orientation of the camera in the scene frame, and  $t$  its position.  $Q_h$  is a 4 dimensional homogeneous vector of a 3 dimensional point in the scene. The matrix  $P$  represent the linear application associated to the projection, its dimension is  $(3 \times 4)$ , and  $q$  is the homogeneous vector associated to the image point of  $Q_h$  by  $P$ .

Identification of matrix  $P$  can be realized by a direct inversion of the system (equation 3). Then we need to know at least the 3D coordinates of 6 points in the scene [15]. Zhang [1] uses homographics properties induced by the use of a planar test pattern in order to identify separately intrinsic and extrinsic parameters. This identification is achieved by the resolution of several linear systems and Ueshiba has shown in [16] that the results are very similar to those we could obtain after a non linear geometric or statistic optimization.

In the following paragraph, this model of camera is improved in order to take care of uncertainty in pixel position.

### B. Pixel model

Algebraic representation of camera model (equation 1) allows us to associate a point in the scene and a point in the image. Nevertheless, data which are furnished by camera are pixels (figure 4-1). The classical mathematical tool used in order to represent this planar aspect is an inaccuracy on real point position. In others words, the exact position of the point has the properties of a Gaussian random variable distributed around the center of the pixel. The deviation of this random variable is characterized by an ellipse which ensures the variable a high probability to be inside the ellipse. Classical choice is  $\sigma = 0.7$ , the ellipse is chosen to ensure a 95% probability to be inside (figure 4-2).

This is a probabilistic model used for geometric computation. One problem is that some hypothesis are imperative to permit the use of such a model. Independence of variables and centered aspect of the distribution are justifiable but false [18]. They allow the use of resolution tools based on quadratic criterions when data are punctual. Concerning sensor calibration (such as cameras), the central limit theorem justifies the probabilistic approach when enough data are available. Then, the punctual results are known with accuracy. But, concerning the triangulation step, this theorem is not justified since only few measurements are used. Triangulation in stereovision is only based one two measures: one points in each image.

According to these approximations, a geometrical approach can be realized using interval analysis. Indeed, we use the alternative proposed in [17] to represent each pixel by an interval (figure 4-3). So, the uncertainty associated to the position of an image point is introduced as the interval  $[\epsilon]$ . This uncertainty has to be considered in the intrinsic parameters. The projection is now written:

$$[q] = E \left( \frac{PQ_h}{P_3^t Q_h} \right) + [\epsilon] \quad (2)$$

Where  $E$  is the round operator which furnishes the nearest integer of a value. The denominator  $P_3^t Q_h$  is the normalization of data description in the image, where  $P_3$  is the third column of the camera model  $P$ . This allows us to fix the scale factor and to define the value of the error vector:  $[\epsilon] = ([\epsilon_1] \ [\epsilon_2] \ 0)^t$ . According to the model, there is no error on the scale factor, but only an uncertainty on the position of the geometric point in the image plane.

If we consider the set of points described by the vector  $[q]$ , they described a planar surface. Thus, an underlying hypothesis traduces an affine model for the camera. Indeed, since the whole set of points included in  $[q]$  is normalized by a unique scale factor ( $P_3^t Q_h$ ), this means that the set of points  $[q]$  is the projection of a set of coplanar points  $\{Q_h\}$ . This hypothesis characterizes an affine functioning of the camera. Nevertheless, in our case, intervals do not describe a set of points  $[q]$  but only one point ( $q$ ) with an unknown but bounded position:  $q \in [q]$ . Thus, the only hypothesis which is made with this description is based on the uncertainty of data according to the model: the uncertainty is bounded.

In a first and empiric approximation, we choose a value for the uncertainty ( $[\epsilon] = ([-0.5, 0.5][ -0.5, 0.5]0)^t$ ) which covers the surface of a pixel. This estimation is sufficient, a method to choose correctly this uncertainty is presented in [17].

In the next section, we present the equation to solve in order to obtain the 3D coordinate of a point from its matched image points. Then we will present the way to solve these equation when points are replaced by pixels. In other words, points are extended with interval analysis information in order to compute the uncertainty of the 3D reconstruction.

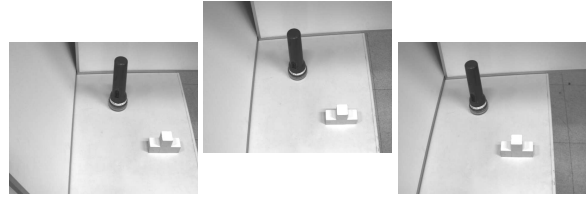


Fig. 5. Original images for 3D reconstruction. 2 kinds of objets are considered: Geometrical form and free form.

### C. 3D reconstruction

The projection which is realized by the camera can be describe algebraically in projective space as a not full rank linear transformation [19][15]. The rank propertie causes the perspective effect. The formation of an image with such a camera is written :

$$q = PQ_h \quad (3)$$

Concerning a stereoscopic system, a couple of camera compensates the not full rank relation in this algebraic representation. Indeed, the relation between a 3D point and its couple of projections provides the following over-determined system:

$$\begin{pmatrix} q_l \\ q_r \end{pmatrix} = \begin{pmatrix} P_l \\ P_r \end{pmatrix} Q_h \quad (4)$$

We observe 6 equations and 4 unknown data. It represents the intersection of the two reprojected lines defined by the center of each camera and each image point. The resolution of this linear system furnishes the coordinate of the 3D reconstructed point. It is equivalent to an overdetermined system in the form:

$$AQ_{nh} = B \quad (5)$$

Matrix  $A$  and vector  $B$  will be given. They are build with the elements of  $P_l, P_r, q_l$  and  $q_r$ .  $Q_{nh}$  is the non homogeneous vector of the 3D point in the scene. Due to the projective representation of space, it is given up to a scale factor [10][19][15].

### D. Uncertainty of data

The method proposed in [10] allows to compute the uncertainty of image point position. It proposes to describe pixel position with intervals ( $[q_l], [q_r]$ ). Then it gives the system (equation 5) from interval arithmetics rules: let us cut the matrix  $P$  associate to a camera model such as:

$$P = (M \mid V) \quad (6)$$

Where  $M$  is a  $(3 \times 3)$  matrix and  $V$  is a  $(3 \times 1)$  vector. The operator  $[*]_{\times}$  is the anti-symmetrical matrix associate to the cross product function. The system (equation 5) is given with the interval matrix  $[A]$  and the interval vector  $[B]$ :

$$[A] = \begin{pmatrix} [[q_l]_{\times} M_l \\ [[q_r]_{\times} M_r \end{pmatrix}; [B] = \begin{pmatrix} [[q_l]_{\times} V_l \\ [[q_r]_{\times} V_r \end{pmatrix} \quad (7)$$

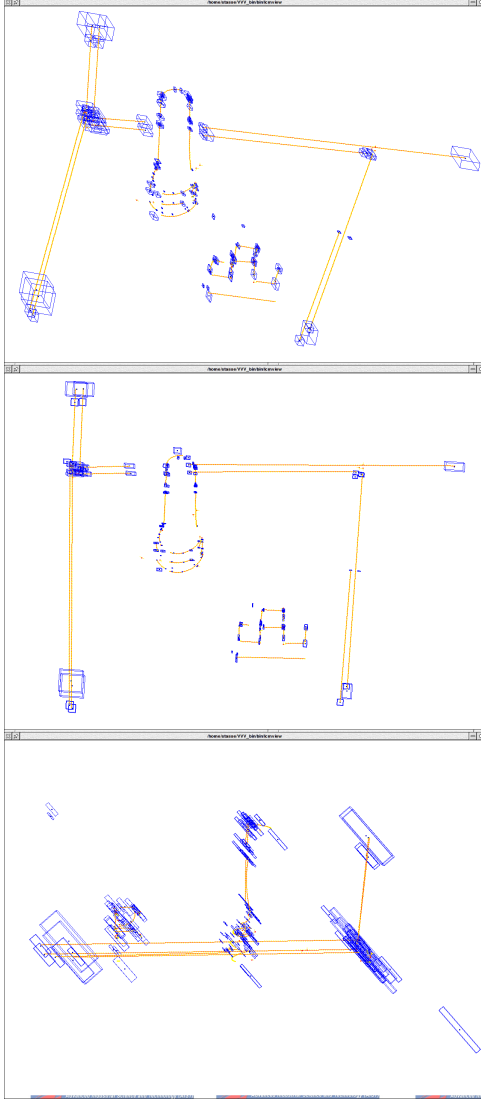


Fig. 6. Different viewpoints of the 3D reconstruction with Boundaries representation and interval bounding boxes. (top-(a), middle-(b), bottom-(c))

The exact set of 3D points  $\{Q_s\}$  which is solution of the uncertain linear system  $[A]Q_{nh} = [B]$  is :

$$\{Q_s\} = \{Q_{nh} \in \mathbb{R}^3 | \exists A \in [A], \exists B \in [B], AQ_{nh} + B = 0\} \quad (8)$$

In the next section we present tools of interval analysis which permit to find a minimal external bounding box  $[X] = [\{Q_s\}]$  of  $\{Q_s\}$ .

#### IV. INTERVAL ANALYSIS

##### A. Uncertain linear system and CSP

We show that the seek of the bounding box  $[X] = [\{Q_s\}]$  with interval analysis is similar to a constraint satisfaction problem (CSP)[20]. Indeed, it is known that lines 3 and 6 of matrix  $A \in [A]$  are linearly dependant [15]. Then, system define by  $[A]$  and  $[B]$  is reduced to dimension  $(4 \times 3)$ . By extracting one more line in this system, we obtain 4 square systems. Since we propose to produce a solution as an external bounding box for each

system, the intersection of solutions provide by each of them is still an external bounding box. For this reason, the next developpements are proposed with square matrix  $[A]$ .

Let us call  $[a_{ij}], [b_i], [x_j]$  the respective elements of matrix  $[A]$  and vectors  $[X]$  and  $[B]$ . The bounding box of the set (equation 8) is produced from the CSP:

$$i = 1 \dots 3, j = 1 \dots 3 : \\ H = \left( \begin{array}{l} \mathcal{X} = \{a_{ij}, b_i, x_j\} \\ \mathcal{D} = \{[a_{ij}], [b_i], \mathbb{IR}^3\} \\ \mathcal{C} = \{f_i : b_i = \sum_{k=1}^{k=3} a_{ik}x_k\} \end{array} \right) \quad (9)$$

Where the set of variable  $\mathcal{X}$  is defined on sets of definition domains  $\mathcal{D}$  and linked by the set of constraints  $\mathcal{C}$ .

Consider the set of variables  $\mathcal{X}$  linked by relations in the form  $f_i(x_j) = 0, i = 1 \dots m, j = 1 \dots n$ . Each variable is known to belong to a domain  $\mathcal{D}_j$ . In the next section, we present fixed point contractors. In interval analysis this operator aims to reduce the width of the intervals  $[x_j]$  according to the set of relations defined by functions  $\{f_i\}$  [10][21]. More generally speaking, this problem is known as the problem of consistence in Constraint Satisfaction Problem (CSP).

##### B. Fixed point contractor

Fixed points contractors are iterative process based on the fixed point theorem [22]. Let us write the evolution of the domain  $\mathcal{D}$  with the serial:

$$\mathcal{D}_{k+1} = \mathcal{R}(\mathcal{D}_k) \quad (10)$$

The operator  $\mathcal{R}$  is the contractor. Let us suppose this serial converge to an optimal or incompressible box  $\mathcal{D}_k$ , then the serial define in (10) reaches to a fixed point and we observe an idempotent phenomena:

$$\mathcal{D}_{k+1} = \mathcal{R}(\mathcal{D}_k) = \mathcal{D}_k \quad (11)$$

Such convergence can be finite or asymptotical according to the system considered. This more precise formalism of the contraction process is defined in [23] and based upon the lattice theory [24]. Thus, an operator for which it exists a solution  $\mathcal{S}$  for the CSP  $H = (\mathcal{X}, \mathcal{D}, \mathcal{C})$ , is a contractor if it verifies the following properties:

$$\begin{array}{ll} \text{contraction} & : [x] \in \mathcal{D} \Rightarrow \mathcal{R}([x]) \in \mathcal{D} \\ \text{monotony} & : [x] \in \mathcal{D}, [x'] \in \mathcal{D} \\ & \quad [x] \subset [x'] \Rightarrow \mathcal{R}([x]) \subset \mathcal{R}([x']) \\ \text{idempotency} & : [x] = \mathcal{S} \Rightarrow \mathcal{R}([x]) = [x] \end{array} \quad (12)$$

The contraction property is simply obtain with pur sets operators. The following serie is contracting:

$$\mathcal{D}_{k+1} = \mathcal{D}_k \cap \mathcal{R}(\mathcal{D}_k) \quad (13)$$

Monotony is a property of functions defined from the constraints according to the domain of definition. These functions are called *inclusion functions*. In the case of linear functions with only one occurrence of each variable, inclusion functions provided by constraints are monotonic [10]. From those remarks, fixed point contractors are operators build upon idempotency. The Gauss-Siedel [25] and Krawczyk [26] contractors are among them.



a) *The Krawczyk-Newton operator:* With this operator, solving an equation written  $f(X) = 0$  using an idempotent property, involves to build a function ( $X$ ) such as

$$f(X) = 0 \Leftrightarrow \psi(X) = X \quad (14)$$

The point  $X$  such as  $f(X) = 0$  is the fixed point of the serie defined by  $X_{k+1} = \psi(X_k)$ . If this serie converges, then it is towards this point.

For a given function  $f$ , at first it is possible to build the corresponding  $\psi$  function by written:

$$\psi(X) = X - Kf(X) \quad (15)$$

With this definition, the property described by equation 14 is fulfilled. Thus the serie can be written:

$$X_{k+1} = \psi(X_k) = X_k - f(X_k) \quad (16)$$

To get the convergence, a linear operator is used. Here the Jacobian of the function  $f$ , i.e.  $K = J^{-1}$ , gives the Newton resolution method, and a new possible  $\psi$  function is:

$$\psi(X_k) = X_k - J^{-1}f(X_k) \quad (17)$$

The function in which we are interested in is written:

$$f(X) = AX - B \text{ thus } J^{-1} = A^{-1} \quad (18)$$

The following inclusion function is used:

$$[f]([X]) = [A][X] - [B] \quad (19)$$

From this, and according to contraction property 13 the final inclusion function  $\psi$  is deduced. It provides the serie:

$$\begin{aligned} [X]_0 &= ] - \infty; +\infty [ \\ [X]_{k+1} &= [\psi]([X]_k) \\ &= [X]_k \cap ((I - A^{-1}[A])[X]_k + A^{-1}[B]) \end{aligned}$$

In the case of linear system, this operator converges quickly to the fixed point (1 or 10 iterations).

b) *The Gauss Siedel contractor:* This contractor is based upon the method used to solve linear system having the same name. Its extension to interval analysis is presented in [21]. For a system of dimension  $n$ :  $AX - B = 0$ , the matrix  $\Lambda$  is punctual one ( $n \times n$ ), with  $\rho(\cdot)$  the operator returning spectral ray of a matrix. This contractor is given by:

$$\left\{ \begin{array}{l} \Lambda \forall A \in [A] : \rho(\Lambda A - I) < 1 ; [M] = [A] - \Lambda^{-1} \\ [\psi]_k([X]) = [X]_{k-1} \cap \Lambda ([b] - [M][X]_{k-1}) \end{array} \right\} \quad (20)$$

Practically, it can be shown that the solution of the system  $([A], [B])$  is equivalent to the *preconditionned* system  $(A^{-1}[A], A^{-1}[B])$  [10]. Then using  $\Lambda = \text{diag}(A^{-1})$  allows to build simply this contractor. [27] presents different preconditionning methods to improve the results of this contractor.

TABLE I  
TIME MEASUREMENTS USING 2 KINDS OF CONTRACTORS

Contractor	Nb Of Iterations	Time (ms)
Gauss Siedel	10	5.23
	5	2.9
	2	1.05
Krawczyk	10	7.64
	5	4.05
	2	1.89

TABLE II  
PRECISION MEASUREMENTS USING THE GAUSS SIEDEL AND KRAWCZYK CONTRACTORS

Nb Of Iterations	Gauss Siedel	Krawczyk
10	1.003612	1.000000
9	1.004032	1.000000
8	1.008824	1.000000
7	1.065419	1.000004
6	1.760988	1.000203
5	10.747894	1.012403
4	135.660754	1.656179
3	2110.601213	50.573413
2	41863.675373	4268.144590
1	1204492.417910	802289.970149

## V. EXPERIMENTAL RESULTS

The previously presented method has been applied to the scene represented in figure 5. Two kinds of objects have been tested on this scene: a geometrical form object and a free-form one. The geometrical object is a T-shape, while the free-form object is a torch-light. The T-shape object and the torch light are of particular interest as they can be handled by the HRP-2 robot. Applying the presented method gives the 3 images displayed in figure 6.a, 6.b, and figure 6.c. The boxes represent the intervals in which lie the features points.

Figures 6.a and 6.b show that the torch-light is the object for which features (point and segments) are the most precisely detected, i.e. for which the boxes are the smallest. The T-shape object is less well detected, but all the visible edges are salient. Due to the geometric model of the camera, deeper objects, or objects far away from the optical axis intersection are less precisely located, as can be seen in figure 6.c. This is particularly clear for the edges of the desk.

The uncertain linear system resolution has been tested using 2 different contractors: Gauss Siedel and Krawczyk. The time costs are summarized in table I. The computer used for the experiments is a 1.5 Ghz Pentium 4 Intel PC. A precision evaluation for both algorithms is given in table II. In order to compare the algorithms on the same data, the two contractors are computed on the same points and with different number of iterations. The precision is computed in

the following manner: each interval of a point is compared with the one given by the Krawczyk contractor for 10 iterations. The latter one is considered as the reference and the most precise value for a given feature point. A ratio is obtained for each dimension. The average of those three ratios gives to the point a precision related to its location. Finally to get a scalar value for one algorithm and a given number of iterations, a second average is performed on all the feature points. Thus given table I and table II the Krawczyk contractor is more accurate than Gauss-Siedel, but it takes more time to compute.

An other contractor proposed in [28] has been implemented. However the test involving the most efficient step of this contractor is violated every time, and then makes necessary the use of an other algorithm more consuming than Krawczyk [29] and less precise.

## VI. CONCLUSION

This paper presented an application of Interval Analysis in the context of 3D reconstruction. This technique provides guaranteed information on the 3D point location according to the camera model. It has been applied to the VVV system to build a partial object representation based on 3D boundaries.

Such approach is interesting for robotic application where unknown object has to be handled, and for which the construction of a model needs to be performed. For instance, using an incremental approach, the bounding boxes provided by the interval analysis delimit the area where to search feature points. If some points have to be more precisely localized, the robot may change its viewpoint to have most of the model accuracy around the wanted location.

Our future work is to extend this approach using the concepts presented in [30] to control the HRP-2 humanoid robot for building 3D object representation.

## REFERENCES

- [1] Z. Zhang, "A flexible new technique for camera calibration," *IEEE Transaction on Pattern Analysis and Machine Intelligence*, vol. 22(11), no. MSR-TR-98-71, pp. 1330–1334, 2000.
- [2] Zhang, "Determining the epipolar geometry and its uncertainty: A review," *International Journal of Computer Vision*, vol. 27(2), pp. 161–198, 1998.
- [3] C. Zeller and O. Faugeras, "Camera self-calibration from video sequences: The kruppa equations revisited," INRIA, Tech. Rep. RR2793, 1996.
- [4] F.-X. Espiau and P. Rives, "Extracting robust features and 3d reconstruction in water images," in *OCEAN*. Hawaii: MTS/IEEE, 2001.
- [5] G. Borges and M. Aldon, "Robust estimation algorithm for mobile robot localization on geometrical environment maps," *To appear in Robotics and Autonomous Systems*, 2004.
- [6] L. Douadi, "Recalage de nuage de points 3d fournis par un capteur embarqué," Master's thesis, Université Montpellier 2, 2002.
- [7] P. Rives, "Visual servoing based on epipolar geometry," in *International Conference on Intelligent Robots and Systems (IROS)*, Takamatsu, Japan, 2000.
- [8] E. Grossmann and J. S. Victor, "The precision of 3d reconstruction from uncalibrated views," in *British Machine Vision Conference*, 1998.
- [9] B. Telle, M. J. Aldon, and N. Ramdani, "Guaranteed 3d visual sensing based on interval analysis," in *Proceedings IROS*, 2003.
- [10] B. Telle, "Méthode ensembliste pour une reconstruction 3d garantie par stereo vision," Ph.D. dissertation, Université Montpellier II, 2003.
- [11] Y. Kawai, T. Ueshiba, Y. Ishiyama, Y. Sumi, and F. Tomita, "Stereo correspondence using segment connectivity," in *Proc. 14th Int'l Conf. on Pattern Recognition, ICPR'98*, 1998, pp. 648–651.
- [12] K. Kaneko, F. Kanehiro, S. Kajita, K. Yokoyama, K. Akachi, T. Kawasaki, S. Ota, and T. Isozumi, "Design of prototype humanoid robotics platform for hrp," October 2002.
- [13] Y. Sumi, Y. Kawai, T. Yoshimi, and F. Tomita, "Recognition of 3d free-form objects using segment-based stereo vision," in *International Conference on Computer Vision*, 1998.
- [14] Y. Sumi, Y. Y. Ishiyama, and F. Tomita, "Hyper frame vision: A real-time vision system for 6-dof object localization," in *International Conference on Pattern Recognition*, 2002.
- [15] R. Hartley and A. Zisserman, *Multiple View Geometry in Computer Vision*. Cambridge, 2001.
- [16] T. Ueshiba and F. Tomita, "Plane-based calibration algorithm for multi-camera systems via factorization of homography matrices," in *9th International Conference on Computer Vision*, Nice (France), oct. 2003, pp. 966–973.
- [17] B. Telle, M. J. Aldon, K. Yokoi, and F. Tomita, "Coherence of 3d reconstruction," in *submission to IROS 2004*, 2004.
- [18] R. Haralick, "Propagating covariance in computer vision," in *Proceedings of Workshop on Performance Characteristics of Vision Algorithms*, 1996, pp. 1–12.
- [19] O. Faugeras, *Three Dimensional Computer Vision*. MIT press, 1992.
- [20] J. Pearson and P. Jeavons, "A survey of tractable constraint satisfaction problems," Uppsala University, Tech. Rep., July 1997.
- [21] L. Jaulin, M. Kieffer, O. Didrit, and E. Walter, *Applied Interval Analysis*. London: Springer Verlag, 2001.
- [22] L. Brouwer, *Geometry, Analysis, Topology and Mechanics, Collected Works 2.*, h. freudenthal, amsterdam: north-holland ed., 1976.
- [23] W. Older, "Interval arithmetic specification," Computing Research Laboratory, Bell-Northern Research, Tech. Rep. n89032, 1989.
- [24] O. Lhomme, "Contribution à la résolution de contraintes sur les reels par propagation d'intervalles," Ph.D. dissertation, Sophia Antipolis, Nice, France, 1994.
- [25] R. Moore, *Interval Analysis*. Englewood Cliffs: Prentice-Hall, 1966.
- [26] R. Krawczyk, "Newton-algorithmen zur bestimmung von nullstellen mit fehlerschranken," *Computing*, vol. 4, pp. 187–201, 1969.
- [27] R. Kearfott, "Interval computations: Introduction, uses and resources," *Euromath Bulletin*, vol. 2, pp. 95–112, 1996.
- [28] S. M. Rump, "Solving algebraic problems with high accuracy," in *Proc. of the symposium on A new approach to scientific computation*, 1983, pp. 51–120.
- [29] G. Hargreaves, "Interval analysis in matlab," University Of Manchester, Tech. Rep., December 2002.
- [30] E. Marchand and F. Chaumette, *Active Vision for Complete Scene Reconstruction and Exploration*, vol. 21, no. 1, January 1999.